Supplementary Information

for

Ion Specific Effects of Monovalent Cations on Deposition Kinetics of Engineered Nanoparticles onto Silica Surface in Aqueous Media

Ruixing Huang[†], Chengxue Ma[†], Qiang He[†], Jun Ma[‡], Zhengsong Wu[†], Xiaoliu Huangfu[†*]

[†]*Key Laboratory of Eco-environments in Three Gorges Reservoir Region, Ministry of Education, Faculty of Urban Construction and Environmental Engineering, Chongqing University 400044, China*

[‡]*State Key Laboratory of Urban Water Resource and Environment, School of Municipal and Environmental Engineering, Harbin Institute of Technology 150001, China*

*Corresponding authors email:

Dr. Xiaoliu Huangfu hfxl@cqu.edu.cn

Tel: +86-023-6512-0980

Fax: +86-023-6512-0980

Summary

Fifteen pages, including 10 figures, 4 tables and 1text.

Text S1. Theoretical Calculation of Interaction Energy for Deposition of C_{60} and CeO_2 NPs on Silica Surface

1. Theory

The classical DLVO theory is extensively used employed to interpret the deposition behavior of NPs or colloids in electrolyte solutions by quantifying the interactions in the macro-interface of colloids. The calculating the interaction energy when they approached to these three surfaces. The main interactions acting on a NP include the van der Waals interaction energy (V_{VDW}) and the electric double layer interaction energy (V_{EDL}). Thus the total interaction energy (V_T) could be calculated using the following equations:[1]

$$V_{Total} = V_{VDW} + V_{EDL} \quad \text{(S1)}$$

where V_{Total} is the total classic energy for monovalent ion species. V_{VDW} is the van der Waals energy and V_{EDL} is the electric double-layer energy.

$$V_{VDW}(h) = -\frac{A_{123}a_p}{6h(1+14h/\lambda)} \quad \text{(S2)}$$

where A_{123} is Hamaker constant for the deposition of a nanoparticle of composition "1" onto a surface of composition "3" when suspended in a medium "2"; a_p is particle radius. h is surface-to-surface separation distance; λ is characteristic wavelength, 100 nm. V_{EDL} could be calculated by: [2-5]

$$V_{EDL}(h) = 64\pi\varepsilon_0\varepsilon_r a_p (k_B T/ze)^2 \Gamma_1 \Gamma_2 \exp(-\kappa h) \quad \text{(S3)}$$

where ε_0 is dielectric permittivity in vacuum, 8.85×10^{-12} F/m; ε_r is relative dielectric permittivity of solution 78.5; k_B Boltzmann constant, 1.3805×10^{-23} J/K; T is absolute temperature, T=298.15 K; $_z$ counterion valence, z=1; e is electron charge, 1.602×10^{-19}

C; Γ_1, Γ_2 is dimensionless surface potential for particle or collector; κ is inverse Debye length.

$$\Gamma_i = \tanh\left({ze\psi_i}/{4k_BT}\right) \quad \text{(S4)}$$

where ψ_i is surface potential, and the value at low potential for EDL energy calculation is presented in Table S1 and S2.

$$\kappa = \left(\frac{2e^2N_AI}{\varepsilon_0\varepsilon_r k_BT}\right)^{1/2} \quad \text{(S5)}$$

where N_A is Avogadro constant, 6.022×10^{23}; I is ionic strength.

The energy was estimated by invoking the Derjaguin approximation throughout. The detailed definition of the parameters can be found in our previous publication.[5] According to the classic DLVO theory, the VDW and EDL interaction energy for NPs with surface in different cationic solutions with the same valence state should be equal at the same electrolyte concentration. However, significant differences deposition rates of NPs determined for identically valent cations suggested that there are other interactions except the identical classic colloidal interactions; this interaction is defined as the additional short-range repulsion energy in this study.[6]

$$V_{ADD}^{ST}(h) = F_0\pi a_p\delta^2 \exp\left(-\frac{h}{\delta}\right) \quad \text{(S6)}$$

Where F_0 is hydration force constant, and δ is the characteristic decay length. The parameters F_0 and δ control the magnitude and the decay of the potential, respectively. The decay length δ is set as the characteristic hydration diameter of the cations (Rb^+ = 658 pm, K^+ = 662 pm, Na^+ = 716 pm, Li^+ = 764 pm).[6] The amplitude of the hydration interaction, F_0, depends mainly on the type of the cations associated on the particle surface and within the ranges 10^6~5×10^8 N/m^2, was estimated based on the

fitted data in previous publication.[6] Therefore, the modified total interaction energy with consideration of ion specificity was rewritten as:

$$V_{Modified} = V_{VDW} + V_{EDL} + V_{ADD}^{ST} \quad \text{(S7)}$$

In the presence of ion specific effects, the difference in additional energies of cations would lead to different adsorption affinities towards a charged NP surface, and thus change surface potentials differently for four metal cations, as observed in Figure 1. The electrostatic energy can be calculated by using different surface potential values of NPs and silica surface (Table S1 and S2)

Table S1. Zeta potential (mV) of C_{60} NPs, CeO_2 NPs for the calculation of modified DLVO interactions in the presence of different monovalent cations over a range of ionic strength.

NP		**Concentration (mM)**					
Type	**Electrolyte**	**1**	**5**	**10**	**20**	**30**	**50**
C_{60} NPs	$LiNO_3$	-29.9	-28.9	-28.4	-25.7	-21.4	-16.7
	$NaNO_3$	-29.4	-28.6	-26.4	-24.7	-19.8	-15.2
	KNO_3	-29.2	-27.8	-25.4	-23.1	-17.0	-15.7
	$RbNO_3$	-27.9	-25.7	-25.4	-23.7	-16.9	-14.6
CeO_2 NPs	$LiNO_3$	20.0	19.2	18.1	17.2	15.1	11.4
	$NaNO_3$	21.1	20.9	20.7	17.8	17.4	10.9
	KNO_3	22.3	20.5	18.8	16.9	15.9	13.7
	$RbNO_3$	21.1	20.7	17.9	17.1	16.2	11.5

Table S2. Zeta potential (mV) of SiO_2 over a range of ionic strength.

Electrolyte	**Concentration (mM)**						**References**
	1	5	10	20	30	50	
$LiNO_3$	-108.7	-102.0	-95.4	-88.7	-82.1	-71.3	[7]
$NaNO_3$	-102.2	-95.5	-88.9	-82.2	-75.6	-65.0	[7]
KNO_3	-92.4	-87.2	-82.1	-76.9	-71.8	-62.4	[7]

$RbNO_3$	-84.8	-80.1	-75.5	-70.8	-66.2	-57.4	-

2. Calculation of Hamaker Constants

Hamaker constants is calculated by[8]:

$$A_{123} = (\sqrt{A_{33}} - \sqrt{A_{22}})(\sqrt{A_{11}} - \sqrt{A_{22}})$$

Where A_{11}, A_{22}, and A_{33} is the Hamaker constants of "1", "2", and "3" in vacuum, respectively required for use in these equations. A_{123} is the Hamaker constant for the deposition of nanoparticles of composition "1" when suspended in a medium "2" on the surface "3".

Table S3. Hamaker constants for the calculation.

NO.	Hamaker constant	System	Value ($\times 10^{-20}$, J)	References
1	A_{11}-C_{60}	nC_{60}	7.50	Chen K. L[9]
2	A_{11}-CeO_2	nCeO_2	5.57	Israelachvili, J. N.[10]
3	A_{22}	water	3.70	Bergström, L. [11]
6	A_{33}	SiO_2	8.86	Israelachvili, J. N. [12]
7	A_{123}-C_{60}	nC_{60}--water-SiO_2	0.47	Qu. X. L[13]
8	A_{123}-CeO_2	nCeO_2-water- SiO_2	0.46	Fang. J [14]

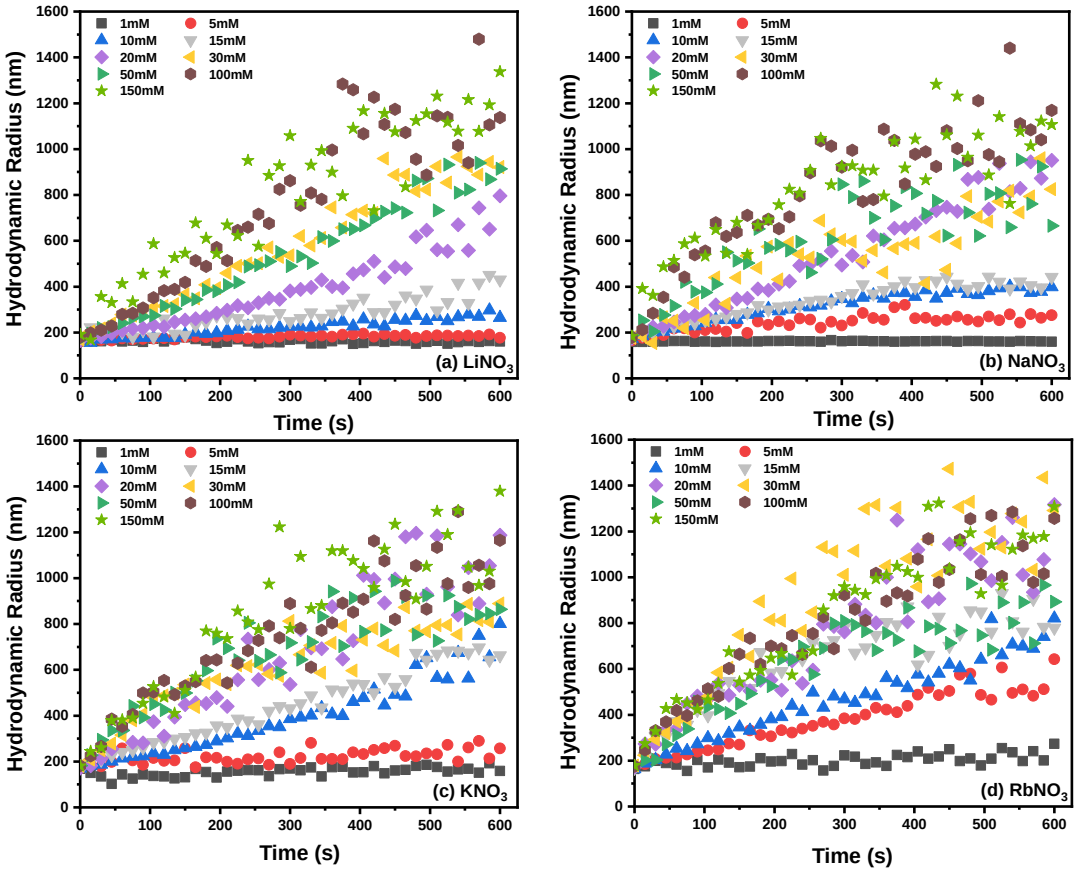

Figure S1. Representative aggregation profiles of C_{60} NPs in the presence of different monovalent ion solutions at pH 6.5 and 25 °C.

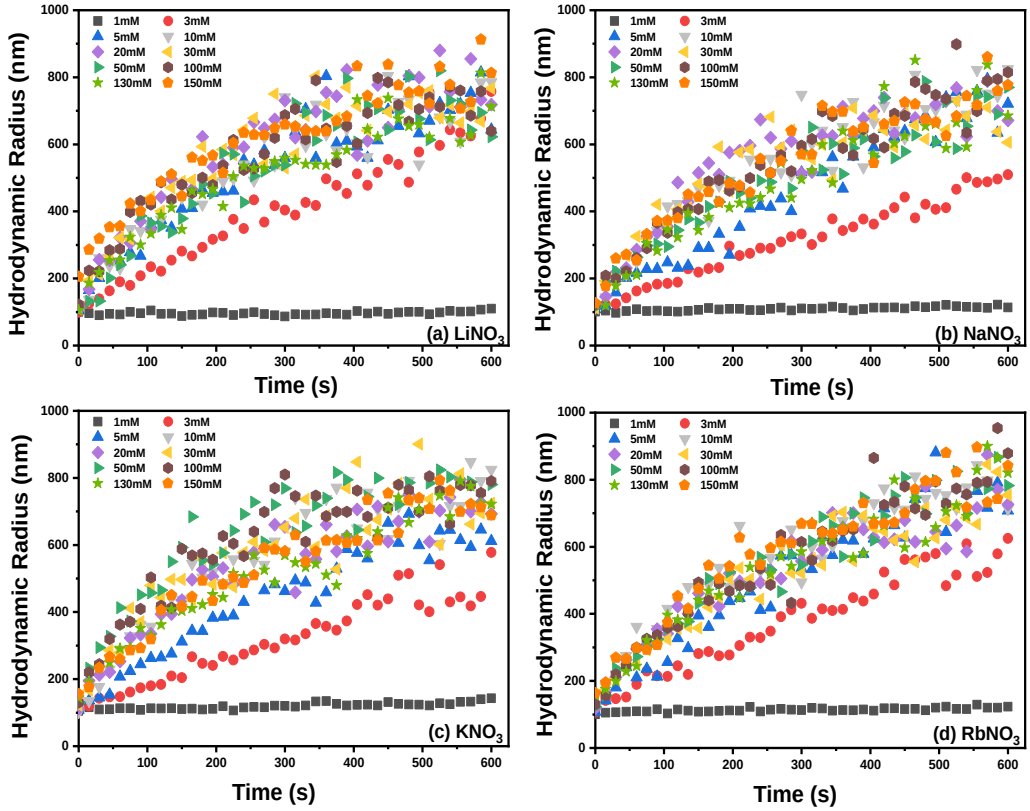

Figure S2. Representative aggregation profiles of CeO_2 NPs in the presence of different monovalent ion solutions at pH 6.5 and 25 °C.

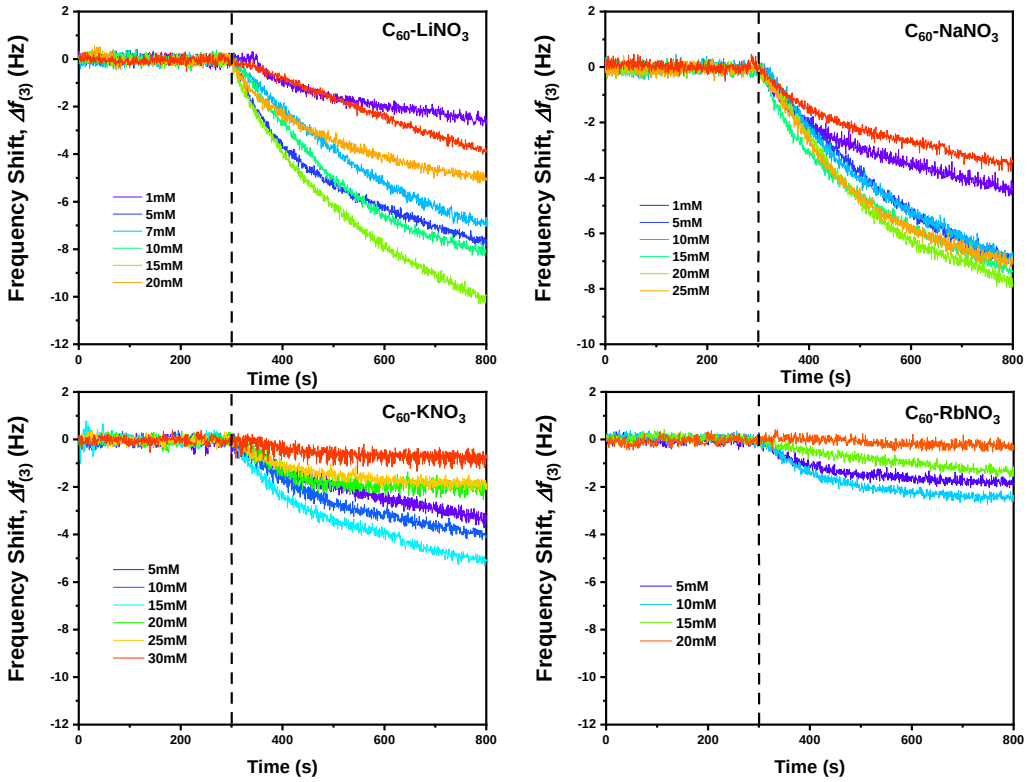

Figure S3. Representative third frequency shift for deposition of C_{60} NPs onto silica coated QCM sensor surfaces in the presence of different monovalent ion solutions at pH 6.5 and 25 ℃.

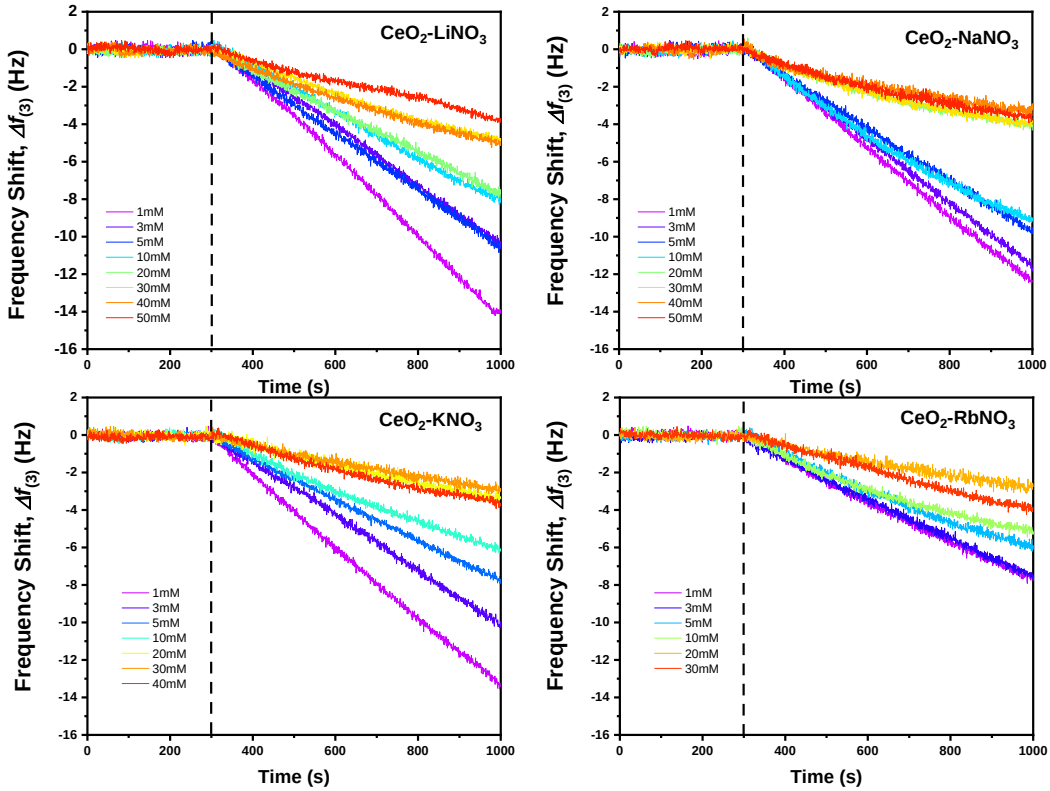

Figure S4. Representative third frequency shift for deposition of CeO_2 NPs onto silica coated QCM sensor surfaces in the presence of different monovalent ion solutions at pH 6.5 and 25 °C.

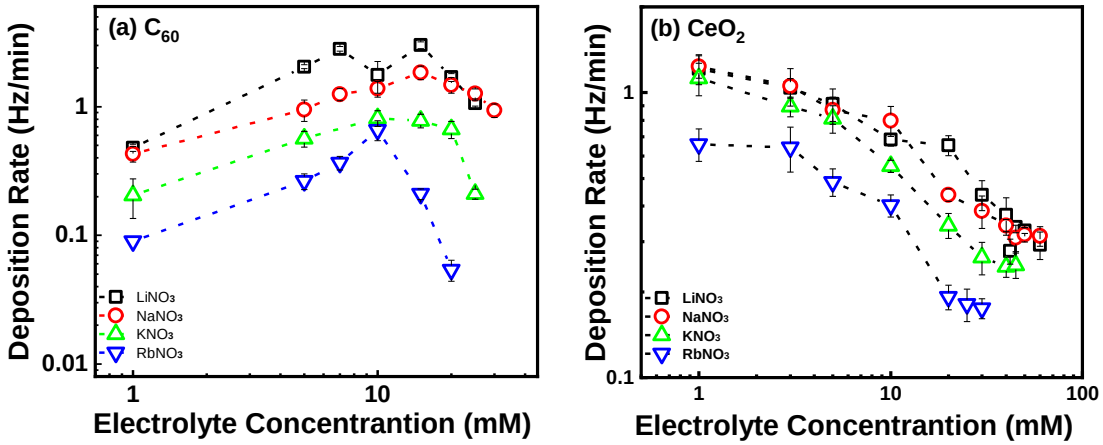

Figure S5. Deposition rate of (a) C_{60} and (b) CeO_2 NPs onto silica coated QCM sensor surfaces as a function of monovalent ion concentration at pH 6.5.

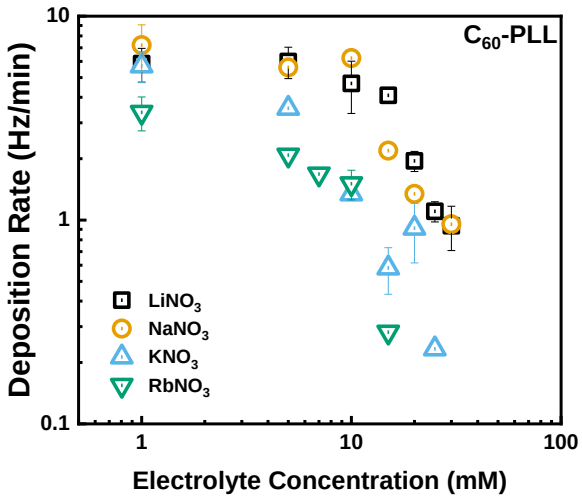

Figure S6. Favorable deposition rates of C_{60} NPs on PLL-coated silica crystal surface as a function of monovalent ion concentration at pH 6.5. Error bars represent standard deviation.

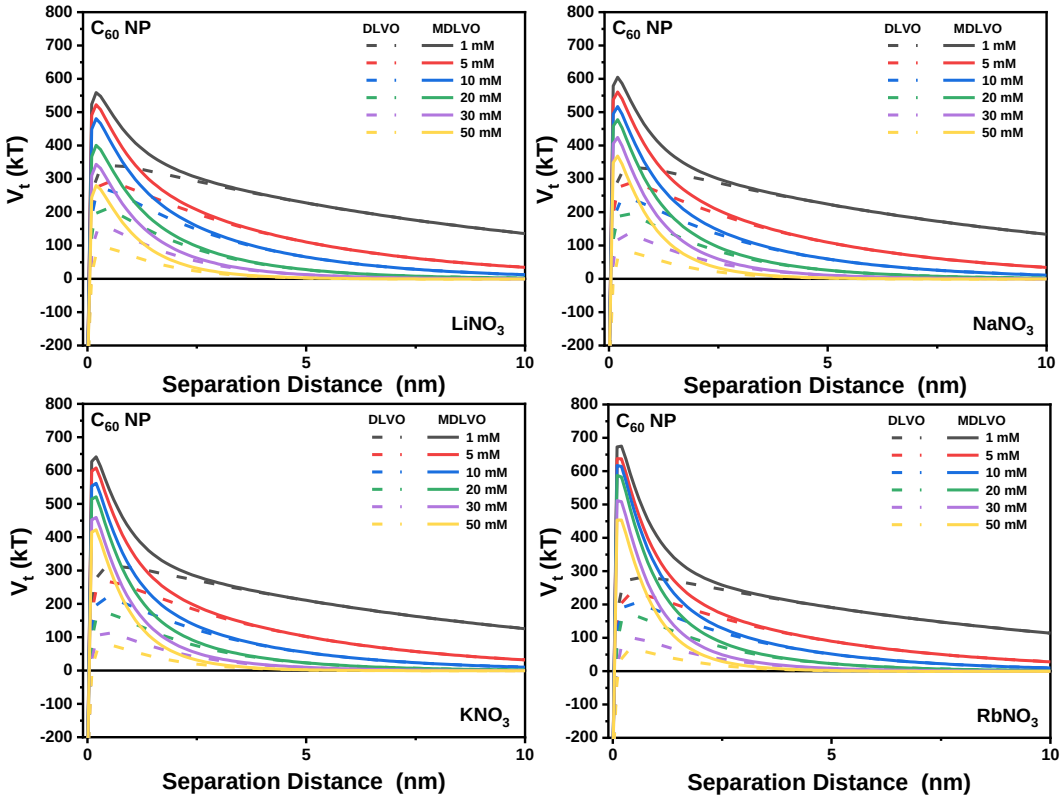

Figure S7. DLVO and MDLVO interaction energy profiles for C_{60} NPs approaching silica surface as function of 1 mM, 5 mM, 10 mM, 20 mM, 30 mM and 50 mM MNO_3 (M= Li^+, Na^+, K^+ and Rb^+) at pH 6.5.

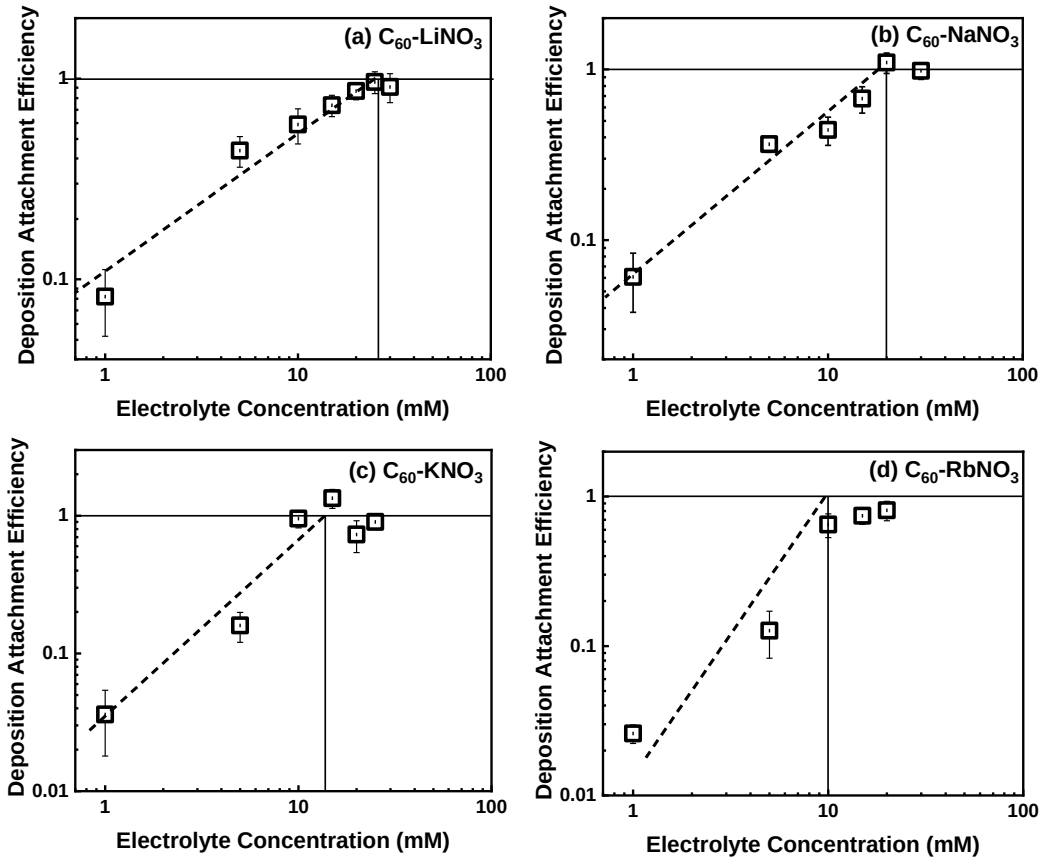

Figure S8. Deposition attachment efficiency of C_{60} NPs as a function of (a) $LiNO_3$, (b) $NaNO_3$, (c) KNO_3 and (d) $RbNO_3$ concentration via normalizing deposition rates to favorable PLL-coated surface at pH 6.5. Error bars represent standard deviations of three runs. The dotted lines are used to schematically indicate the changing trend of deposition attachment efficiency. By extrapolating through the two regimes, the intersections of the extrapolations yield CDCs of 25 mM $LiNO_3$, 20 mM $NaNO_3$, 13 mM KNO_3 and 10 mM $RbNO_3$ for deposition of C_{60} NPs on silica surface.

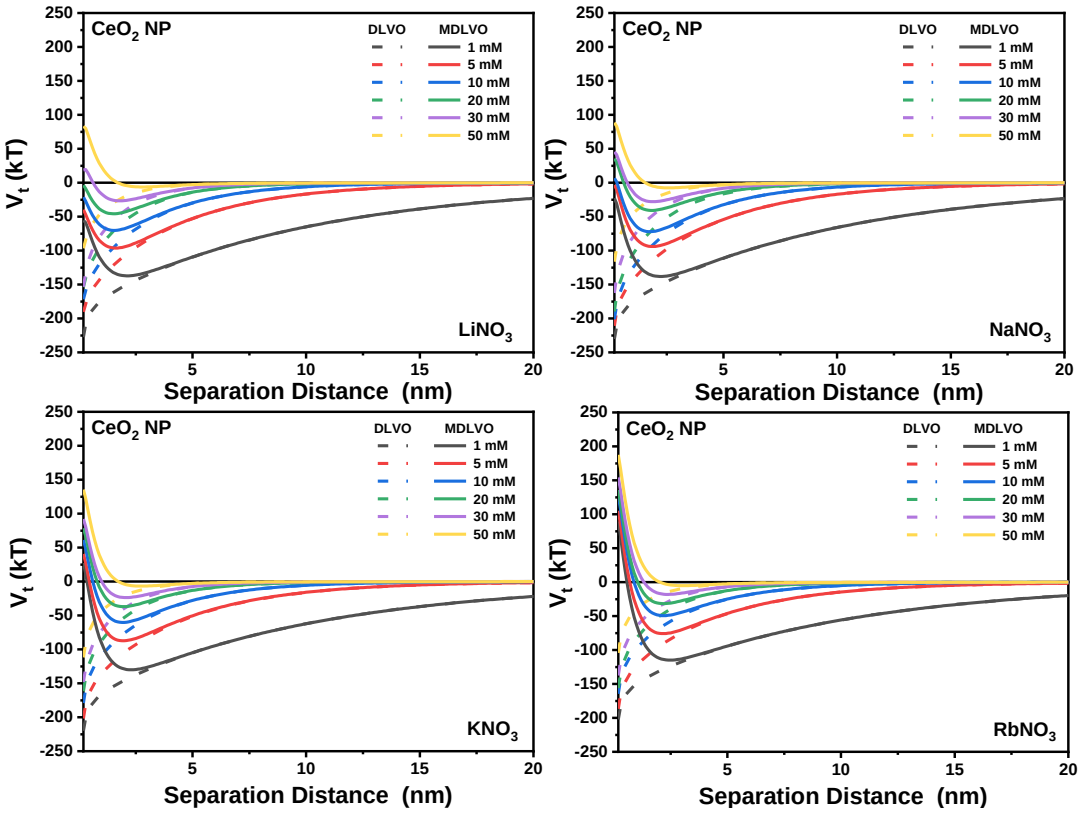

Figure S9. DLVO and MDLVO interaction energy profiles for CeO_2 NPs approaching silica surface as function of 1 mM, 5 mM, 10 mM, 20 mM, 30 mM and 50 mM MNO_3 (M= Li^+, Na^+, K^+ and Rb^+) at pH 6.5.

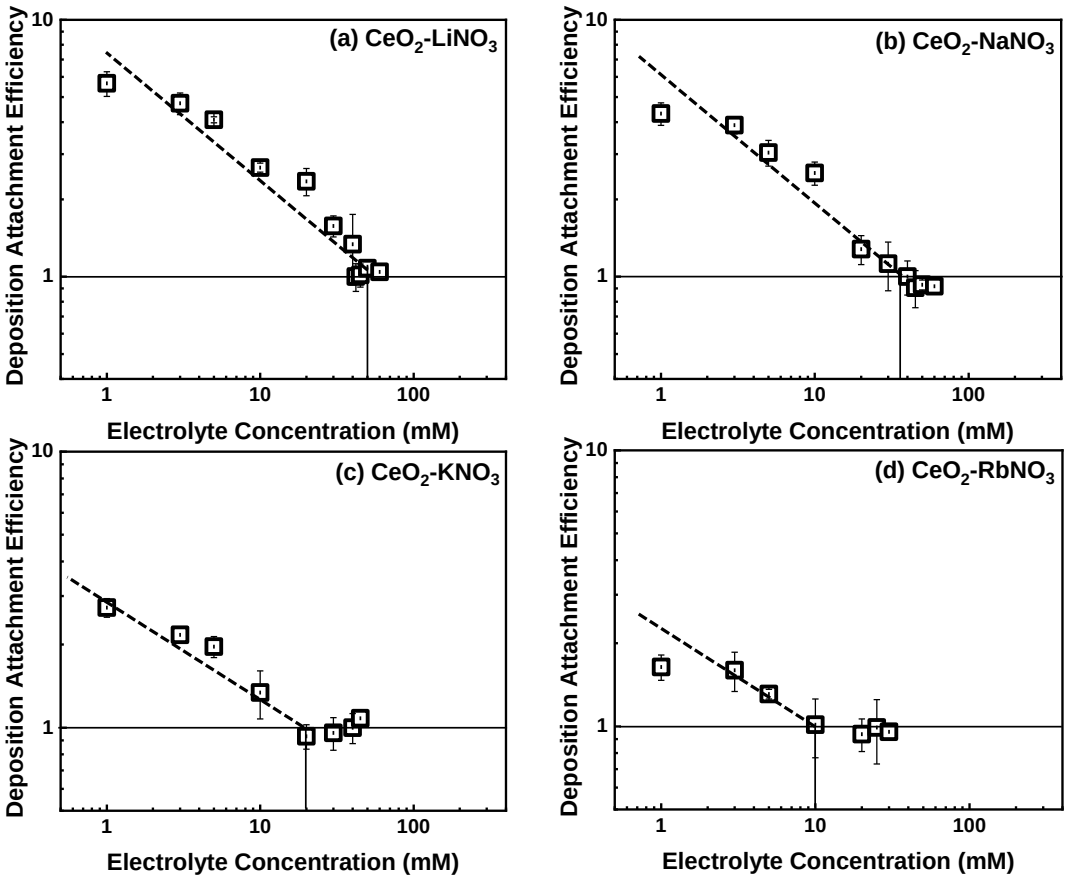

Figure S10. Deposition attachment efficiency of CeO_2 NPs as a function of (a) $LiNO_3$, (b) $NaNO_3$, (c) KNO_3 and (d) $RbNO_3$ concentration via normalizing deposition rates to diffusion controlled deposition rate at pH 6.5. Error bars represent standard deviations of three runs. The dotted lines are used to schematically indicate the changing trend of deposition attachment efficiency. By extrapolating through the two regimes, the intersections of the extrapolations yield CDCs of 43 mM $LiNO_3$, 35 mM $NaNO_3$, 20 mM KNO_3 and 10 mM $RbNO_3$ for deposition of CeO_2 NPs on silica surface.

Table S4. Initial aggregation rates of C_{60} and CeO_2 NPs in the presence of alginate and BSA at the electrolyte of 5 mM.

Nanoparticle	Electrolyte	Aggregation Rate (nms^{-1})		
		NPs only	NPs + Alginate	NPs + BSA
C_{60}	$LiNO_3$	0.12±0.09	0.06±0.03	-
	$NaNO_3$	0.14±0.12	0.09±0.02	0.02±0.01
	KNO_3	0.18±0.06	0.11±0.08	0.05±0.03
	$RbNO_3$	0.54±0.11	0.32±0.10	0.11±0.06
CeO_2	$LiNO_3$	1.44±0.23	0.67±0.22	0.21±0.07
	$NaNO_3$	1.49± 0.31	0.82±0.17	0.18±0.06
	KNO_3	1.35± 0.47	0.54±0.08	0.34±0.05
	$RbNO_3$	1.74±0.11	0.66±0.11	0.29±0.11

REFERENCES

1. A. R. Petosa, D. P. Jaisi, I. R. Quevedo, M. Elimelech and N. Tufenkji, Aggregation and deposition of engineered nanomaterials in aquatic environments: Role of physicochemical interactions, *Environ. Sci. Technol.*, 2010, **44**, 6532-6549.
2. J. GREGORY, Interaction of unequal double layers at constant charge, *Journal of Colloid and Interface Science*, 1975, **51**, 44-51.
3. D. Grasso*, K. Subramaniam, M. Butkus, K. Strevett and J. Bergendahl, A review of non-DLVO interactions in environmental colloidal systems, *Reviews in Environmental Science and Bio/Technology*, 2002, **1**, 17-38.
4. A. Petosa, D. Jaisi, I. Quevedo, M. Elimelech and N. Tufenkji, Aggregation and deposition of engineered nanomaterials in aquatic environments: role of physicochemical interactions., *Environ Sci Technol*, 2010, **44**, 6532-6549.
5. X. Huangfu, C. Ma, R. Huang, Q. He, C. Liu, J. Zhou, J. Jiang, J. Ma, Y. Zhu and M. Huang, Deposition Kinetics of Colloidal Manganese Dioxide onto Representative Surfaces in Aquatic Environments: The Role of Humic Acid and Biomacromolecules, *Environ Sci Technol*, 2018, DOI: 10.1021/acs.est.8b04274.
6. M. van der Linden, B. O. Conchuir, E. Spigone, A. Niranjan, A. Zaccone and P. Cicuta, Microscopic Origin of the Hofmeister Effect in Gelation Kinetics of Colloidal Silica, *J Phys Chem Lett*, 2015, **6**, 2881-2887.
7. A. H. Jalil and U. Pyell, Quantification of Zeta-Potential and Electrokinetic Surface Charge Density for Colloidal Silica Nanoparticles Dependent on Type and Concentration of the Counterion: Probing the Outer Helmholtz Plane, *J Phys Chem C*, 2018, **122**, 4437-4453.
8. M. Elimelech, J. Gregory, X. Jia and R. A. Williams, Particle Deposition and Aggregation: Measurement, Modeling, and Simulation., *Butterworth-Heinemann: Oxford, England*, 1995.
9. K. Chen and M. Elimelech, Aggregation and deposition kinetics of fullerene (C60) nanoparticles, *Langmuir*, 2006, **22**, 10994-11001.
10. J. Israelachvili and H. Wennerström, Role of hydration and water structure in biological and

colloidal interactions, *Nature*, 1996, **379**, 219.

11. L. Bergstr6m, Hamaker constants of inorganic materials, *Advancesin Colloid and Interface Science*, 1997, **70**, 125-169.

12. J. N. Israelachvili, *Intermolecular and Surface Forces*, Academic Press,
London, 2011.

13. X. Qu, P. J. Alvarez and Q. Li, Impact of sunlight and humic acid on the deposition kinetics of aqueous fullerene nanoparticles (nC60), *Environ Sci Technol*, 2012, **46**, 13455-13462.

14. J. Fang, M.-h. Wang, D.-h. Lin and B. Shen, Enhanced transport of CeO 2 nanoparticles in porous media by macropores, *Science of The Total Environment*, 2016, **543**, 223-229.